NREL
NATIONAL RENEWABLE ENERGY LABORATORY

Improved Energy Conversion Efficiency in Wide-Bandgap Cu(In,Ga)Se2 Solar Cells

Preprint

Miguel Contreras, Lorelle Mansfield,
Brian Egaas, Jian Li, Manuel Romero,
and Rommel Noufi
National Renewable Energy Laboratory

Eveline Rudiger-Voigt and Wolfgang Mannstadt
Schott AG

Presented at the 37th IEEE Photovoltaic Specialists Conference (PVSC 37)
Seattle, Washington
June 19-24, 2011

Conference Paper
NREL/CP-5200-50669
July 2011

Contract No. DE-AC36-08GO28308

NOTICE

Available electronically at http://www.osti.gov/bridge

Available for a processing fee to U.S. Department of Energy
and its contractors, in paper, from:

U.S. Department of Energy
Office of Scientific and Technical Information

P.O. Box 62
Oak Ridge, TN 37831-0062
phone: 865.576.8401
fax: 865.576.5728
email: mailto:reports@adonis.osti.gov

Available for sale to the public, in paper, from:

U.S. Department of Commerce
National Technical Information Service
5285 Port Royal Road
Springfield, VA 22161
phone: 800.553.6847
fax: 703.605.6900
email: orders@ntis.fedworld.gov
online ordering: http://www.ntis.gov/help/ordermethods.aspx

Cover Photos: (left to right) PIX 16416, PIX 17423, PIX 16560, PIX 17613, PIX 17436, PIX 17721

Printed on paper containing at least 50% wastepaper, including 10% post consumer waste.

IMPROVED ENERGY CONVERSION EFFICIENCY IN WIDE BANDGAP $Cu(In,Ga)Se_2$ SOLAR CELLS

Miguel A. Contreras[1], Lorelle M. Mansfield[1], Brian Egaas[1], Jian Li[1], Manuel Romero[1], Rommel Noufi[1]
Eveline Rudiger-Voigt[2], Wolfgang Mannstadt[2]
[1]National Renewable Energy Laboratory, Golden, CO, USA
[2]Schott AG, Mainz, Germany

ABSTRACT

This report outlines improvements to the energy conversion efficiency in wide bandgap (E_g>1.2 eV) solar cells based on $CuIn_{1-x}Ga_xSe_2$. Using (a) alkaline containing high temperature glass substrates, (b) elevated substrate temperatures 600˚C-650˚C and (c) high vacuum evaporation from elemental sources following NREL's three-stage process, we have been able to improve the performance of wider bandgap solar cells with 1.2<E_g<1.45 eV. Initial results of this work have led to efficiencies >18% for absorber bandgaps ~1.30 eV and efficiencies ~16% for bandgaps up to ~1.45 eV. In comparing J-V parameters in similar materials, we establish gains in the open-circuit voltage and, to a lesser degree, the fill factor value, as the reason for the improved performance. The higher voltages seen in these wide gap materials grown at high substrate temperatures may be due to reduced recombination at the grain boundary of such absorber films. Solar cell results, absorber materials characterization, and experimental details are reported.

INTRODUCTION

$CuIn_{1-x}Ga_xSe_2$ (CIGS)-based solar cells have achieved the highest energy conversion efficiency (>20%) among photovoltaic (PV) thin-film materials. Those solar cells are typically made from CIGS alloys with low Ga content (x~0.3) resulting in absorber energy bandgap values ~1.1-1.2 eV. It is desirable to develop wider bandgap absorbers for a variety of reasons and not just to tune E_g to 1.4 eV, as suggested by the theoretical calculations for optimum conversion efficiency.

In practice, low E_g solar cells suffer from a great loss of power output when their operating temperature becomes >>25˚C. This is referred to as the thermal coefficient of efficiency (or power) loss and sometimes is quoted as a percentage loss of power (or voltage) in commercial modules. Crystalline silicon (E_g~1.1 eV), for example, has a -0.50%/˚C efficiency loss, which is a little worse than CIGS at -0.44%/˚C (Eg~1.2 eV). On the other hand, other thin-film PV technologies like a-Si and CdTe (E_g~1.45 eV) show coefficients of power/efficiency loss of -0.17%/˚C and -0.25%/˚C respectively. Since modules under real operating conditions can get as hot˚Cas 50 -75˚C depending on location and evidently time of the year, it means that the efficiency (or power output) of low bandgap cells and modules are effectively de-rated by at least 11% and in some instances as high as 25%. It is also desirable to have solar cells (and modules) that produce higher output voltages and a lower current (as wider gap solar cells should) in order to minimize the intrinsic resistive losses ($R*I^2$) in a module or cell.

As mentioned above, historically the high efficiency regime for CIGS has been limited to the low E_g materials and efficiencies attained for CIGS materials with E_g>1.2 eV have been low [1,2]. In this paper, we report on recent improvements to CIGS materials with E_g>1.2 eV and discuss the solar cell parameters, processes, and materials physical properties that have enabled high efficiency (>15%) for E_g values (so far) up to ~1.45 eV.

CIGS GROWTH AND SOLAR CELL FABRICATION

The *standard* growth of high efficiency CIGS thin-films requires the use of high substrate temperatures (~600C) and a clear correlation between this parameter and the performance attained from those films has been established: in brief, the higher the substrate temperature the better the performance, see for instance ref [3]. The CIGS community has been limited to the use of soda-lime glass (SLG) or stainless steel as a substrate choice for reasons of cost, but such substrates also limit the degree of freedom in this important parameter. In such substrates, processing temperatures of 550C or less are commonly used to avoid deformation and/or adhesion problems in the case of the glass or to limit the diffusion of unwanted impurities from the steel into the CIGS absorber film. Other glasses and oxides, such as borosilicate glass (BSG) or alumina plates have been used in CIGS R&D, but the lack of sodium and a non-optimum thermal coefficient of expansion relative to the Mo back contact make them a less attractive choice.

The development and availability of a high temperature glass tailored to CIGS technological needs, such as: (1) a much higher softening point than that of SLG, (2) a matching of the thermal coefficient of expansion to the Molybdenum back contact, and (3) a source of sodium, has enabled a revisit of the CIGS performance for 0<x<1 with an emphasis on x>0.3. We have studied the behavior and quantified the performance of solar cells fabricated on SCHOTT specialty glass. And, we have used the NREL three-stage process for the fabrication of the absorbers and selected substrate temperatures in the range of 600˚C to 650˚C. In the following sections, we will refer to the CIGS materials obtained in this study as *high temperature* CIGS to help in our presentation of data and discussion.

All solar cells fabricated have a standard ZnO/CdS/CIGS/Mo layered structure where the molybdenum back contact of the solar cells is deposited by DC sputtering; the CdS by chemical bath deposition and the ZnO by RF sputtering from ceramic targets. The small area (~0.4 cm^2) solar cells fabricated in this study also incorporate a top contact grid with ~5% obscuration loss made of nickel and aluminum and deposited by electron beam evaporation. Selected champion solar cells were coated with an antireflection layer of MgF_2.

SOLAR CELL RESULTS

CIGS solar cells made in this study were analyzed by current density-voltage (J-V), external quantum efficiency (EQE) and capacitance-voltage (C-V) measurements. The J-V characteristics obtained for the many cells (>300) fabricated in this work are perhaps best summarized by *certified* J-V measurements for a selected few champion cells made with high temperature absorbers of varied absorber bandgap values (see Fig.1). Additionally, Table I shows the main J-V parameters for selected solar cells from this study. For comparison, Fig.1 includes the efficiency values published in the literature for other related works in this area of wide gap chalcogenides (references [4,5,6,7,8,9]). The energy bandgap values for the NREL data in Fig. 1 were determined from quantum efficiency (QE) curves by arbitrarily assigning an "effective" bandgap value to the energy calculated from the wavelength value where a 20% QE value is observed for the long wavelengths.

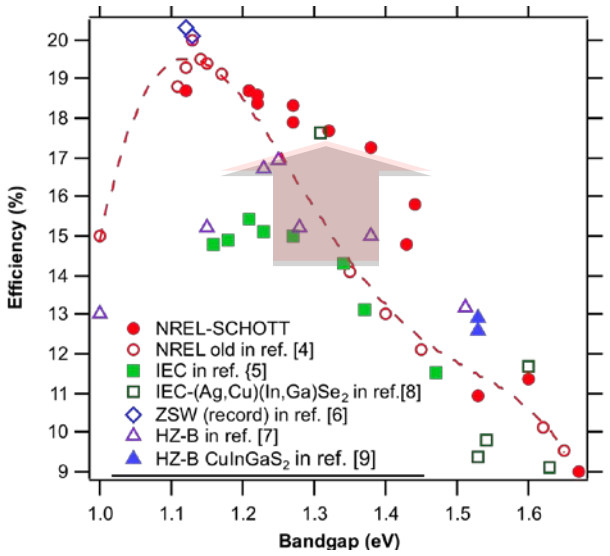

Figure 1 Solar cell efficiency vs. CIGS absorber bandgap value.

From the J-V parameters obtained, we can attribute the enhancement in performance for CIGS solar cells with 1.20 eV<E_g<1.45 eV to the attainment of higher open-circuit voltage (V_{oc}) values as shown in the graph of V_{oc} vs. E_g in Fig. 2. The data in Fig. 2 show not just the higher absolute values for the voltage but also:

(a) an improvement to the (expected) linear behavior of V_{oc} as a function of E_g for solar cells with energy gaps in the range 1.10 eV<E_g<1.35 eV

(b) the breakdown of that linear behavior of V_{oc} as a function of E_g for solar cells with E_g>1.35 eV

(c) a saturation of the V_{oc} values at ~830 mV for solar cells with E_g>1.35 eV.

Table I. J-V parameters of high temperature wide gap CIGS solar cells.

V_{oc} (V)	J_{sc} (mA/cm^2)	FF (%)	Efficiency (%)	E_g (eV)
0.743	31.9	78.75	18.7	1.21
0.752	31.2	77.73	18.3	1.27
0.801	28.5	77.21	17.7	1.32
0.817	27.5	76.65	17.2	1.38
0.801	24.4	75.55	14.8	1.43
0.813	26.9	72.17	15.8	1.44
0.829	20.2	65.32	11.0	1.53
0.766	20.9	71.02	11.4	1.60
0.795	16.4	69.22	9.0	1.67

The fill factor values (FF) and their trend with of E_g (or Ga content) for the high temperature CIGS solar cells are not any different than those values seen in standard CIGS. The maximum FF values (77%-79%) are attained for bandgaps 1.20 eV<E_g<1.35 eV and for higher energy gap values the FF values decrease gradually to values ~70% for E_g~1.67 eV (or x=1.0) in the pure $CuGaSe_2$ case.

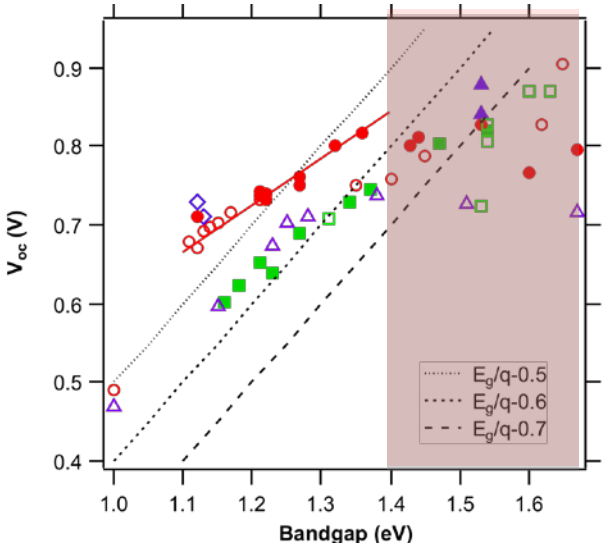

Figure 2 V_{oc} vs. CIGS absorber bandgap value. Data symbols as noted in Fig.1.

Similarly to the FF data, the short-circuit current density (J_{sc}) of the high temperature CIGS solar cells do not differ from what has been seen and reported for standard CIGS absorber materials: our experimental J_{sc} values do follow the expected linear behavior of decreasing J_{sc} values with increased bandgap (or Ga content).

The EQE data for selected devices for which the absorber layers were grown at the highest substrate temperatures of this study (T_s~650˚C) are shown in Fig.3. The insert in the figure shows the CIGS absorber *bulk* atomic chemical composition (x) values that were obtained by x-ray fluorescence (XRF) analysis. It is important to note that when using the NREL three-stage evaporation process, and due to the different diffusivity values for In and Ga, a direct correlation of bandgap to bulk Ga content is not quite correct because of the graded bandgap nature of those films. We find a more realistic estimate of an *effective* bandgap value for three-stage CIGS films can be obtained from QE data and in a manner explained earlier: 20% QE value in long wavelengths (shown by the small arrow in Fig. 3 for the pure $CuGaSe_2$ case).

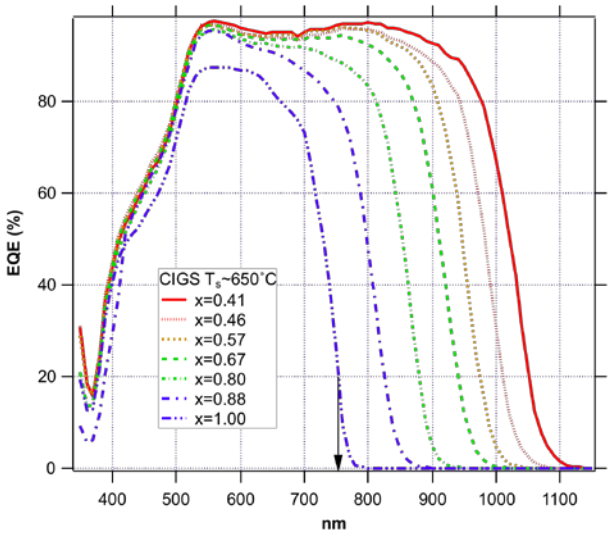

Figure 3 External quantum efficiency curves for CIGS solar cells with absorbers grown at 650˚C.

From the EQE data, another shortcoming of the wider gap CIGS solar cells is revealed: as the Ga content is increased, the overall collection of the cells decreases predominantly for the longer wavelengths indicative of reduced diffusion lengths in those cells. In other words, photons that penetrate deep into the wide gap absorber are not contributing effectively to current generation and are lost to recombination. The highest bandgap materials, such as the $CuGaSe_2$ case in Fig.3, also show an overall lower collection efficiency (<90%) in the visible wavelengths, an indication additional recombination is further limiting the performance of such cells.

It was mentioned earlier that the gains in efficiency reported in this work for high temperature CIGS solar cells with 1.2 eV<E_g<1.45 eV were due to higher voltages as compared to results from standard CIGS absorber materials. For this reason, it became imperative in our work to establish any significant or measurable differences in the diode behavior and the absorber physical properties of high temperature and standard CIGS samples fabricated in the course of this work.

From C-V and dark J-V measurements on selected solar cells, we were able to establish two important observations about these devices:

(a) the carrier concentration values—C-V data not shown—for these new high temperature CIGS absorbers are similar to that of earlier CIGS materials. On the other hand,

(b) the diode reverse saturation current density (J_o) for these new high temperature absorbers is measurably and significantly lower (by more than 1 order magnitude) than values seen previously in materials with similar bandgap values.

Fig. 4 shows the dark J-V curves for representative CIGS wide gap solar cells with E_g~1.5 eV from this study illustrating the lower J_o values in solar cells made with high temperature wide gap CIGS absorbers. The lower values measured in the J_o parameter for such cells is significantly lower for materials with 1.2 eV<E_g<1.5 eV; however, in solar cells made with high temperature CIGS and E_g>>1.5 eV the J_o values are similar to those in standard CIGS materials with similar bandgaps.

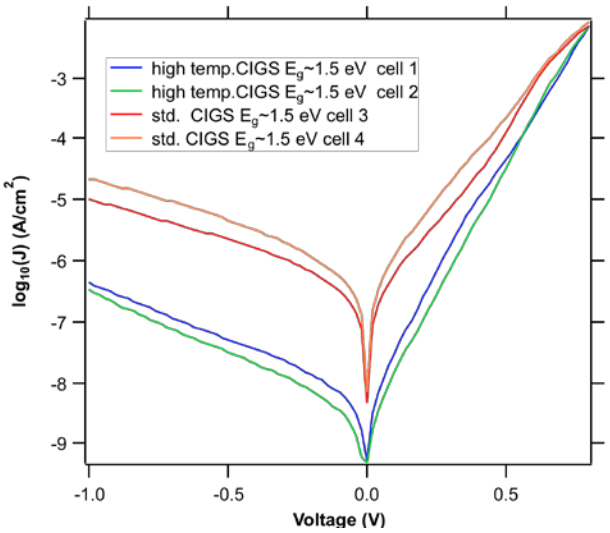

Figure 4 Dark J-V curves for high temperature CIGS (lower curves) and standard CIGS (upper curves) solar cells with Eg ~1.5 eV.

HIGH TEMPERATURE CIGS ABSORBER CHARACTERIZATION

Because of the interesting features seen in J-V, C-V, EQE and room temperature dark-JV data of the solar cells made with high temperature CIGS, we investigated several physical properties of the CIGS absorbers used in those cells and compared data and observations to standard CIGS materials in order to establish more differentiating characteristics between materials.

The chemical composition of the CIGS absorbers fabricated were characterized by XRF, Auger electron spectroscopy (AES) and secondary ion mass

spectroscopy (SIMS). Morphological and structural information was obtained from scanning electron microscopy (SEM) and x-ray diffraction (XRD). Lastly, cathode luminescence (CL) spectroscopy and imaging were also carried out on representative samples to study grain boundary phenomena [10].

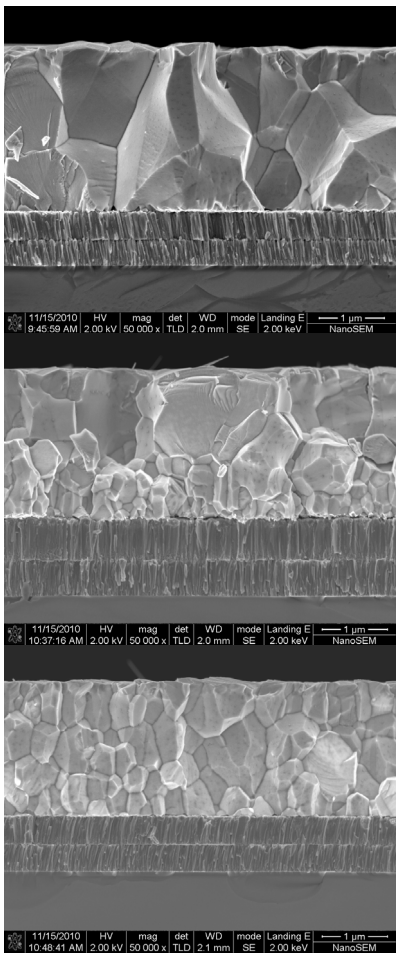

Figure 5 Morphology of CIGS grown at 650 ˚C for x~0.4 (top), x~0.5 (middle) and x=1 (bottom).

Let us begin with microstructure and morphological observations. Here, the SEM data indicates there is a reduction in grain size as Ga content is increased (for the same substrate temperature). Even the highest substrate temperatures in our experiments (650˚C) fail to achieve grain sizes that are of the order of film thickness (~2 µm) for Ga contents above x~0.5. The morphology of CIGS with x>0.5 is characterized by small grain size in the back of the film (near the Mo layer) and larger grains towards the surface. Eventually, for x>0.9 the films become homogeneous in grain size but with submicron grain sizes. Figure 5 shows three representative CIGS materials grown at ~650˚C depicting these morphological differences.

From XRD data (not shown), we establish that all films grown in this study have a preferential orientation in the (220) direction. The use of higher than standard processing temperatures does not seem to hinder this structural characteristic and, in fact, high temperature CIGS films are highly textured in that crystallographic orientation. On the other hand, the high processing temperatures lead to more uniform films in terms of chemical composition regarding the Ga content. That is, the graded bandgap nature of three-stage films is less pronounced as the substrate temperature is increased. In other words, the typical "notch" shape to the Ga profile seen in compositional depth profiles such as those obtained from SIMS and/or AES becomes less prominent (see Fig.6).

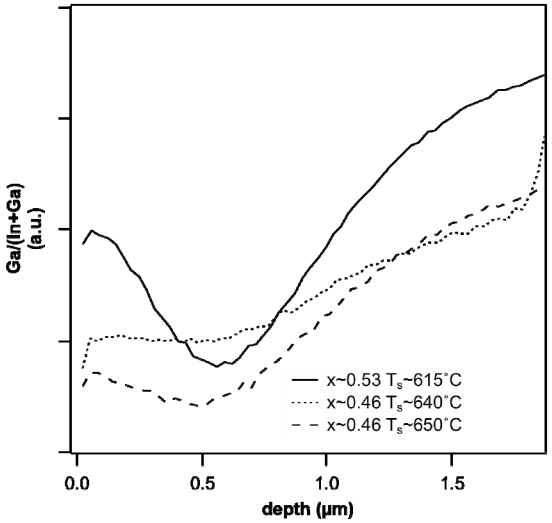

Figure 6 SIMS Ga/(In+Ga) ratio as a function of film depth.

Structural and chemical properties of the high temperature CIGS materials are not different than expected from the three-stage process and the effect of higher processing temperatures. But the grain boundary (GB) activity we see and report here from CL measurements is in our experience something new in these materials.

From our earlier work on CL as applied to wide bandgap materials, we learned that the elevated temperatures help in minimizing a certain pair of radiative defect states with an emission localized 1.41-1.46 eV within the gap of materials such as pure $CuGaSe_2$ [11]. The wide-gap high temperatue CIGS materials reported here lack that particular emission and we can assert that those defect levels have been reduced. Additionally, when we look at the GB CL emission, we find the high tenperature CIGS materials have emissive properties at the GB similar to those we have previously associated with high efficiency materials [12, 13]. That is, all high efficiency CIGS materials we studied in the past displayed what we have previously refered to as the "red shift" in the GB CL emission (relative to the CL emission at the grain interior)

of such materials: there is a small, yet measurable shift in the donor-to-acceptor (DAP) emission peak intensity energy towards lower energy emission values, hence, “red shift” (as shown in Fig. 7). We have previously associated this CL emission shift with the precense of a large neutral barrier leading to reduced recombination at the GB.

(a)

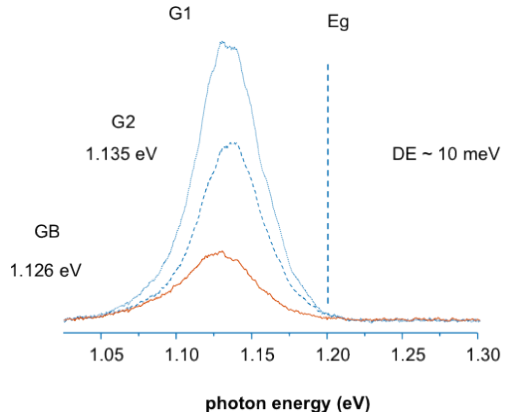

(b)

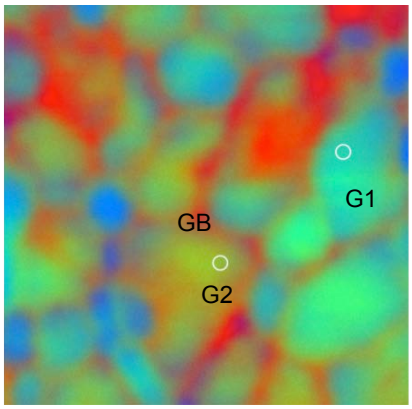

Figure 7 Typical CL emission (a) linescan and (b) energy map at 1.130 eV, 80 meV energy window at grain interior (G1,G2) and at GB in high efficiency CIGS.

In the past, we only observed that behaviour for standard low Ga-content CIGS materials with bandgaps <1.2 eV and higher E_g standard CIGS materials did not show this ”red shift” behavior; that is, the energy of the GB emission did not differ significantly from that of the grain interior (see Fig. 8). The high temperature CIGS solar cells we report here do show such “red shift” in the CL emission at their grain boundaries as can be seen from the CL photon energy maps we obtained for a selected number of high temperature (and standard) CIGS materials. Figures 7-9 show the spectra and CL energfy maps (color coded) for three cases that exemplify our findings.

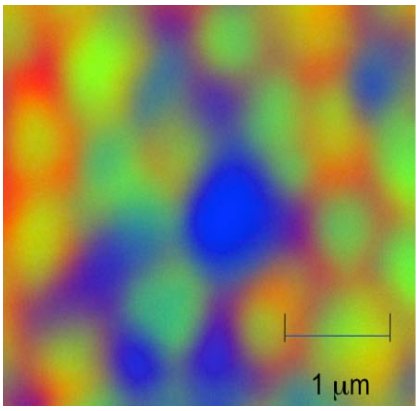

Figure 8 Energy map map of the CL emission (at 1.260 eV, 80 meV energy window) from standard CIGS with x~0.60 from year 2003.

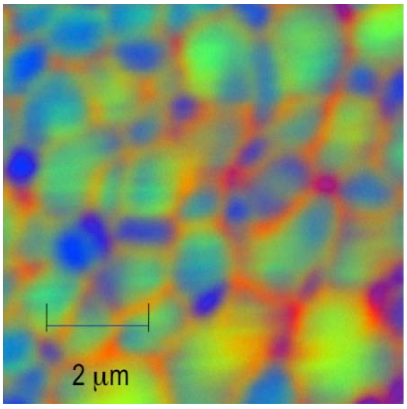

Figure 9 Energy map of the CL emission from high temperature CIGS with x~0.60 (similar conditions as in Fig.8 were used).

DISCUSSION

Considering standard solar cell equations and based on data presented above, we can deduce that the higher voltages seen in the high temperature CIGS solar cells arise from a reduced reverse saturation current density value and not to an increase of carrier concentration. It is also clear to us that the grain boundary activity in high temperature CIGS absorber materials has been improved and now match the behavior seen in standard high efficiency solar cells. As an upshot, we can say that the defects present at grain boundary of these new materials provide for a reduced recombination at grain boundary. The true nature of those *beneficial* defects at the grain boundary may still be a matter of discussion but whatever their nature is, we are inclined to think they are the main reason for the improvements to wider gap CIGS solar cells reported here.

We note that the “red shift” is present in all samples fabricated, even in the widest bandgap materials such as $CuGaSe_2$. However, as it has been shown, the solar cells with E_g>1.45 eV still suffer from a limited value in V_{oc}. It is

very likely other limiting factors are present (aside from grain boundary recombination) that limit the V_{oc} of the widest gap materials (E_g> 1.45 eV). We speculate that factors such as band alignment between the CdS and the wider gap CIGS materials may not be optimum and perhaps alternatives to CdS, wider gap "buffer" layers may be needed to discern more limiting factors of the widest gap solar cells (E_g>1.5 eV). There could be other reasons as well, such as the nature of the electrical conductivity type at the usually Cu-depleted surface region of these materials. Naturally, more investigations are necessary, but within the scope of this work we can already see and report significant improvements to the performance of wide gap CIGS solar cells.

CONCLUSIONS

We have experimented with higher than standard substrate temperatures for the growth of CIGS materials with 0.3<x<1.0. The much more elevated processing temperatures than the standard 550˚C-600˚C typically used have led to significant improvements to wide gap CIGS solar cells with bandgaps up to 1.45 eV. The main parameter that has improved is the output voltage of the cells as compared to previous (and standard) CIGS materials. A reduction in the reverse saturation current density value is responsible for the enhanced voltages attained. The high temperature CIGS materials grown show improvements to their grain boundary characteristics and now show properties similar to those found in high efficiency CIGS materials with low bandgaps (E_g<1.2 eV). The widest bandgap solar cells (Eg >1.5 eV) are still limited in performance (efficiency <15%). Additional experimental and theoretical work are necessary to finally isolate and identify the most significant limiting factors in the efficiency and voltage for those solar cells.

ACKNOWLEDGEMENT

This work was supported by the U.S. Department of Energy under Contract No. DE-AC36-08-GO28308 with the National Renewable Energy Laboratory. Also, many thanks to our colleagues at NREL: Ingrid Repins, Bobby To and Paul Ciszek for data and input to this work.

REFERENCES

[1] R. Herberholz, V. Nadenau, U. Rühle, C. Köble, H.W. Schock , B. Dimmler. *Solar Energy Materials and Solar Cells* **49**, 1997, pp. 227-237.

[2] M. Gloeckler and J.R. Sites. *Thin Solid Films*, Volumes **480-481**, 1 June 2005, Pages 241-245.

[3] Li Zhang, Qing He, Wei-Long Jiang, Fang-Fang Liu, Chang-Jian Li, Yun Sun. *Solar Energy Materials & Solar Cells* **93**, 2009, pp. 114–118.

[4] Miguel A. Contreras, K. Ramanathan, J. AbuShama, F. Hasoon, D. L. Young, B. Egaas and R. Noufi. *Prog. Photovolt: Res. Appl.,* 2005; **13**, pp. 209–216.

[5] W.N. Shafarman, R. Klenk, and B.E. McCandless. *Twenty fifth IEEE PVSC*, 1996; pp. 763.

[6] P. Jackson, D. Hariskos, E. Lotter, S. Paetel, R. Wuerz, R. Menner, W. Wischmann and M. Powalla. Twenty fifth EU PVSEC, WCPEC-5, Valencia, Spain, 2010.

[7] T. Eisenbarth, T. Unold, R. Caballero, C.A. Kaufmann, D. Abou-Ras, H.-W. Schock. *Thin Solid Films* **517**, (2009) 2244–2247.

[8] G. M. Hanket, J. H. Boyle, and W. N. Shafarman. "Characterization and device performance of (Ag,Cu)(In,Ga)Se_2 Absorber layers", *IEEE PVSC*, 2009, pp. 1240.

[9] S. Merdes, R. Mainz, J. Klaer, A. Meeder, H. Rodriguez-Alvarez, H.W. Schock, M.Ch. Lux-Steiner, R. Klenk. "12.6% efficient CdS/Cu(In,Ga)S2-based solar cell with an open circuit voltage of 879 mV prepared by a rapid thermal process", *Solar Energy Materials & Solar Cells* **95** 2011, pp. 864–869.

[10] M. J. Romero, K. Ramanathan, M. A. Contreras, M. Al-Jassim, R. Noufi, P. Sheldon. *Appl. Phys. Lett*. **83**(23), 4770 (2003).

[11] M. A. Contreras, M. Romero, and D. Young, "Optimization of $CuGaSe_2$ for Wide-bandgap Solar Cells", Proceedings of the 3rd World Conference in Photovoltaic Energy Conversion, Osaka, Japan.

[12] M. A. Contreras, I. Repins, W. K. Metzger, M. Romero and D. Abou-Ras, "Se activity and its effect on Cu(In,Ga)Se_2 photovoltaic thin films", *Phys. Status Solidi A 206*, No. **5**, 1042–1048 (2009).

[13] M. A. Contreras, M. J. Romero, R. Noufi, "Characterization of Cu(In,Ga)Se_2 materials used in record performance solar cells", *Thin Solid Films* **511–512** (2006), pp. 51–54.